

Article

Flowable Electrodes from Colloidal Suspensions of Thin Multiwall Carbon Nanotubes

Massinissa Hamouma¹, Wilfrid Neri¹, Xavier Bril¹, Jinkai Yuan^{1,2} , Annie Colin³, Nicolas Brémond⁴ 
and Philippe Poulin^{1,*} ¹ University Bordeaux, CNRS, CRPP, UMR 5031, 33600 Pessac, France² LCMCP, Sorbonne Université, UMR 7574, 75005 Paris, France³ MIE, CBI, ESPCI Paris, Université PSL, CNRS, 75005 Paris, France⁴ LCMD, CBI, ESPCI Paris, Université PSL, CNRS, 75005 Paris, France

* Correspondence: philippe.poulin@crpp.cnrs.fr

Abstract: Flowable electrodes, a versatile alternative to traditional solid electrodes for electrochemical applications, exhibit challenges of high viscosity and carbon content, limiting flow and device performances. This study introduces colloidal suspensions of thin multiwall carbon nanotubes (MWCNTs) with diameters of 10–15 nm as electrode materials. These thin nanotubes, stabilized in water with a surfactant, form percolated networks, exhibiting high conductivity (50 ms/cm) and stability at a low carbon content (below 2 wt%). Colloidal clustering is enhanced by weak depletion attractive interactions. The resulting suspensions display yield stress and a shear thinning behavior with a low consistency index. They can easily flow at a nearly constant shear over a broad range of shear rates. They remain electrically conductive under shear, making them a promising option for flow electrochemical applications. This work suggests that the use of depletion-induced MWVNT aggregates addresses crucial issues in flow electrochemical applications, such as membrane fragility, operating energy, and pressure. These conductive colloidal suspensions thereby offer potential advancements in device performance and lifespan.

Keywords: carbon nanotubes; conductivity; flow electrochemistry; depletion



Citation: Hamouma, M.; Neri, W.; Bril, X.; Yuan, J.; Colin, A.; Brémond, N.; Poulin, P. Flowable Electrodes from Colloidal Suspensions of Thin Multiwall Carbon Nanotubes. *Colloids Interfaces* **2024**, *8*, 32. <https://doi.org/10.3390/colloids8030032>

Academic Editor: István Szilágyi

Received: 26 March 2024

Revised: 13 May 2024

Accepted: 16 May 2024

Published: 17 May 2024



Copyright: © 2024 by the authors. Licensee MDPI, Basel, Switzerland. This article is an open access article distributed under the terms and conditions of the Creative Commons Attribution (CC BY) license (<https://creativecommons.org/licenses/by/4.0/>).

1. Introduction

Flowable electrodes are emerging as a versatile and promising alternative to traditional solid electrodes in various electrochemical applications, including flow capacitors [1–3] and water capacitive desalination [4–6]. Flow capacitors enjoy several promising features such as cost effectiveness and high-energy storage capabilities. More critically, flow electrochemical technologies offer the possibility to decouple energy and power ratings. The energy scales with the volume of the reservoirs, whereas the charge transfer depends on the structure and stacks of the device. These features make flow capacitors and flow batteries particularly suited for storage of intermittent renewable energies. Flowable electrodes are also promising to address an environmental concern that is the global water resource shortage [7]. The so-called flow capacitive deionization of water using carbon slurry was already introduced in 2013 [8] and has been a topic of extensive research since then [9–11]. Moreover, flow capacitive water desalination has been shown to be potentially more effective by implementing energy recovery during continuous deionization process [12].

In these applications, which are based on related physico-chemical mechanisms, carbon micro- or nanoparticles [2] are suspended in an electrolyte medium, often containing formulating agents [13,14]. At elevated concentrations, the colloidal particles create an electrically conductive network [15]. Upon the application of a given voltage, ions from the volume of the electrolyte adsorb onto the particle surface during the charging stage. Conversely, electrical charges are delivered to a current collector in the discharge mode. In contrast to their solid counterparts, flowable electrodes offer numerous advantages, such as

a high surface area accessible from the entire electrolyte volume, enhanced mass transport, and ease of replacement. Flowable electrodes in these applications generally contain a high amount of carbon particles to ensure electrical conductivity. High concentration yields viscoelastic suspensions, with a slurry like texture, impeding easy flow. They necessitate high pressure and energy to be pumped. More critically, a high concentration of carbon particles can result in plug formation or membrane rupture, limiting the performance and lifespan of devices [11]. This can become critical when using ion exchange membranes, which are costly components of energy storage or deionization devices.

To overcome these limitations, an approach consists of developing flowable electrodes with reduced carbon content. Reducing carbon content holds the potential for improving device stability, prolonging lifespan, and enhancing energetic efficiency. The first challenge towards this objective involves optimizing the rheological performance of carbon dispersions. Maintaining the dispersion's ability to flow is crucial. The second challenge is to formulate flowable dispersions that still exhibit sufficient electronic conductivity and electrochemical capacitance. Generally, as reviewed in references [3,16], carbon-based slurries made of carbon black particles display conductivities below a few mS/cm, for carbon contents of the order of 10 wt% or more. Moreover, the conductivity of such slurries decreases sometimes substantially in flow conditions.

A way of maintaining conductivity over a wide shear rate range is by utilizing a fluid that can accommodate high shear rates with limited viscous dissipation. This is particularly the case of threshold fluids with low plastic viscosity or, more precisely, with a low consistency index and a high yield stress. Their equation of state is $\sigma = \sigma_s + A\dot{\gamma}^n$, where A is the consistency index, σ_s the yield stress, σ the applied shear stress, $\dot{\gamma}$ the shear rate, and n the flow index [17]. In the limit of low A , the applied stress is maintained around the yield stress. The apparent viscosity, defined as $\eta_{app} = \frac{\sigma}{\dot{\gamma}} = \frac{\sigma_s}{\dot{\gamma}} + A\dot{\gamma}^{n-1} \approx \frac{\sigma_s}{\dot{\gamma}}$, varies with the shear rate to the power of -1 . Flow in such fluids generally occurs through minute structural variations, characterized by fractures that continuously form and heal, especially as the fluid flows in close proximity to its yield stress. Such a behavior is usually observed at low shear rates in yield stress fluids with high carbon contents [3,18,19]. Achieving such flow conditions over a broad range of shear rates and at low carbon contents remains challenging.

Carbon nanotubes appear as natural candidates to meet the above challenges. Indeed, carbon nanotubes display a high conductivity [20] and a low percolation threshold at equilibrium because of their high aspect ratio, L/d , where d and L are the diameter and length of the nanotubes, respectively [21]. They hold therefore the potential for making conductive suspensions at a low carbon content. Actually, such particles have been used as additives, mixed with other carbon particles, to improve capacitive water desalination performances [22–24]. Nanotubes contribute to generate connectivity between the carbon particles. They have also been used as sole conductive species in aqueous electrodes with remarkable properties [16,25,26]. In these earlier studies, electronic conductivities at equilibrium reached values between 5 and 10 mS/cm for carbon contents typically between 2.5 and 10 wt%. These remarkable properties result from the high conductivity of carbon nanotubes and from their high aspect ratio. Nevertheless, nanotubes used in these studies have a diameter of 50–80 nm and a length of 10 μ m. Stabilization of such particles remains quite difficult because of their large size and tendency to settle. In addition, the large size of the particles results in a more limited specific surface area and electrochemical capacitance compared to smaller colloidal nanoparticles.

Following the investigation of carbon nanotube-based flowable electrodes, we report in the present work the obtainment of electrodes made of suspensions of thin multiwall carbon nanotubes (MWCNTs) with a diameter of 10–15 nm. Even if not as good as activated carbons in terms of performances for static supercapacitors, they are expected to display greater capacitance compared to thick nanotubes. These thinner nanotubes do not settle and can be more easily dispersed than large multiwall nanotubes. The nanotubes are stabilized in water with surfactant. Addition of excess surfactant is used to promote the

formation of percolated networks in response to weak depletion attractive interactions [27]. We perform characterizations following the methodology used for carbon black particles [3]. In this previous work, conductivity measurements and rheology characterizations were conducted. The methodology also includes the measurement of conductivity in flow cells as detailed in [3] and in the Materials and Methods Section of the present article. However, the present work is focused on fundamentally distinct materials since carbon black is made of aggregates of quasi-spherical particles. Here, carbon nanotubes are 1 D dimensional objects with a high aspect ratio. They form structures different from carbon black systems. The present structures are shown to display high conductivity and high stability along with decent electrochemical capacitance. Typically, the best dispersions investigated in the present work display an electronic conductivity of 50 ms/cm for a carbon content below 2 wt%. The viscosity of these suspensions does not exceed 2 Pa.s for a shear rate of 5 s⁻¹. This original combination of high electronic conductivity and low plastic viscosity makes the present suspensions promising for flow electrochemical applications where membrane fragility, operating energy, and pressure are key issues.

2. Materials and Methods

Two types of commercial multiwall carbon nanotubes have been used, namely, Graphistrength C100 materials from Arkema (Colombes, France) and NC 700 materials from Nanocyl (Sambreville, Belgium). These nanotubes are produced by a chemical vapor deposition process and contain small fractions of metal catalysts. They are used as received without further purification. Both materials have diameters in the 10–15 nm range. According to statistical analyses of the correlation between the diameter and number of nanotube walls, this diameter range corresponds typically to a number of walls varying between 10 and 15 [28]. The nanotube length exceeds several microns in their raw state.

The carbon nanotubes are added to distilled water and stabilized with surfactant molecules. US4498 from US Research Nanomaterials is presently used. The exact molecular structure of the surfactant is unknown, but the compound is provided by US Research Nanomaterials as a non-ionic surfactant suited for the stabilization of carbon nanotubes in water. This surfactant contains aromatic groups with good affinity towards carbon nanotubes. As a non-ionic molecule, the surfactant is not expected to affect the ionic conductivity of the suspensions. However, surfactant molecules adsorbed at the surface of the nanotube can increase the contact resistance between the particles. This effect would likely lower the overall electronic conductivity of the suspension. Mother suspensions are prepared by mixing 1 wt% of MWCNTs and 2 wt% of US4498 in distilled water for Arkema samples and 0.5 wt% of MWCNTs and 2 wt% of US4498 for Nanocyl samples. The suspensions are homogenized by tip sonication for 30 min. They are obtained using a Branson homogenizer, Sonifier model S-250A (Fisher Scientific, Leicestershire, UK), associated with a 13 mm step disruptor horn and a 3 mm tapered microtip, operating at a 20 kHz frequency. The suspensions are found to be free of aggregates after such treatment. Tip sonication induces the disentanglement and scission of the nanotubes [29,30]. The latter display a typical length in the range of 500 nm–1 μm. Transmission electron micrographs of isolated MWCNTs after sonication are shown in Figure 1.

The mother suspensions are then further concentrated by dialysis. This is achieved by placing the suspensions in Spectra/Por dialysis membrane bags with a 6–8 kD molecular weight cut-off. This cut-off allows the transport of water and surfactant molecules, but the membranes retain MWCNTs. The dialysis bags are placed in contact with a Spectra/gel absorbing hydrogel. Water and surfactant molecules are adsorbed by the gel, and the concentration of MWCNTs in the dialysis bag increases with time. The concentration of surfactant also increases nearly similarly because of its much lower diffusion compared to that of water molecules. Using aqueous solutions of surfactants, we have actually verified that the transport of surfactants across the membrane is negligible on the time scale of the present experiments. Typically, the surfactant concentration is found to increase almost linearly with the reduction in volume of the solution. The ratio of surfactant to MWCNTs

can therefore be considered to be constant when the total concentration of dried materials increases. Varying the time of dialysis allows different concentrations of MWCNTs to be achieved. The amount of dried materials, including surfactant and MWCNTs, contained in the suspensions is measured by dry extract experiments. The weight fraction of MWCNTs is deduced from the known initial ratio of surfactant to MWCNT. The most concentrated samples investigated in the present work have a MWCNT weight fraction above 4 wt% obtained after 6 h of dialysis.

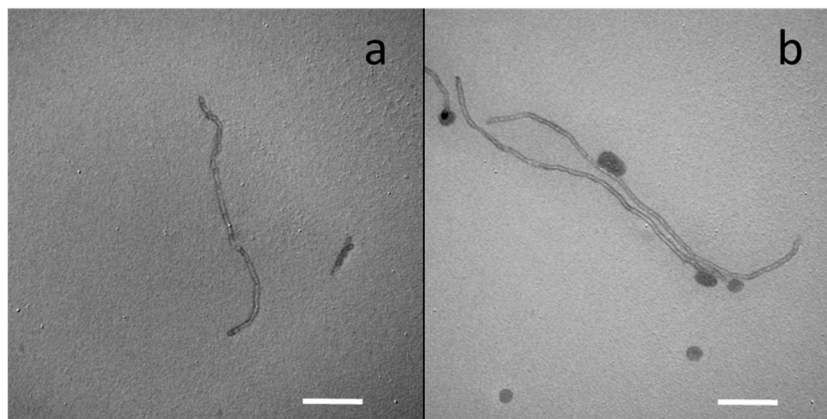


Figure 1. Transmission electron micrographs of individual Arkema (a) and Nanocyl (b) MWCNTs after sonication. Scale: 100 nm.

The phase behavior of the samples is assessed by optical microscopy using a Leica DM2500 microscope.

The conductivity of the samples at equilibrium is measured using a Radiometer CDC749 conductivity cell connected to a Keithley 2000 multimeter. A constant voltage of 0.5 V is applied between the electrodes of the cell, and the current is measured as a function of time. The current decreases until it reaches a stationary value, typically after a few minutes. The stationary current corresponds to the contribution of electronic conductivity of the samples, without the contribution of ionic conductivity [31]. Conductivity is measured at a room temperature of 20 °C. It is anticipated that increasing the temperature could result in an increase in conductivity via thermally induced tunneling, as commonly observed in nanocomposite systems [32]. However, actual experiments would be required to confirm the effect.

Conductivity in shear flow is measured using a Couette cell (Caplim Rheophysique West 3400) as detailed in [3]. In the present work, conductivity is measured in the radial direction of the Couette cell with two concentric circular electrodes. The conductivity corresponds to the conduction in the shear plane, perpendicular to the flow direction.

The rheological properties are characterized by an AR1000 controlled stress rheometer from TA Instrument (New Castle, DE, USA). A ramp of shear rate is applied from 200 s⁻¹ to 0.1 s⁻¹, with 5 points per decade. Each shear rate is maintained for 30 s, and the viscosity is measured by averaging the measurements over the last 5 s. The temperature is set with a Peltier system at 20 °C.

The electrochemical capacitance of the suspensions is measured in a two-electrode symmetric cell configuration. The setup is described in detail in [3]. The liquid electrodes have the same volume and are separated from each other by using an anion exchange membrane (SnakeSkin[®] Dialysis Tubing 1000 MWCO, Fisher Scientific). Cyclic voltammetry is performed using an Autolab PGSTAT204 Metrohm potentiostat/galvanostat (Metrohm Autolab Inc., Utrecht, The Netherlands).

3. Results and Discussion

Optical micrographs of MWCNT suspensions are shown in Figure 2 for Arkema samples and in Figure 3 for Nanocyl samples. It is observed in both cases that aggregates tend to form with the increasing concentration of MWCNTs and surfactant in the suspensions. This aggregation behavior is ascribed to depletion attraction between the nanotubes due to the presence of surfactant micelles [27,33]. Depletion attraction is weak [34] and results in loose aggregates that do not settle with time. The aggregates remain in constant equilibrium with dispersed and individualized nanotubes.

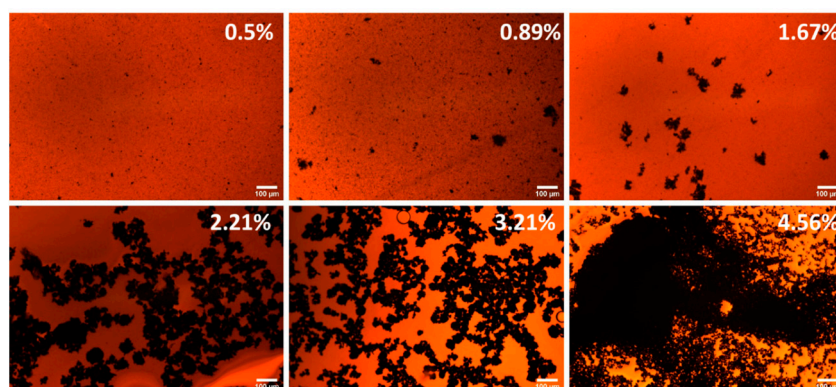


Figure 2. Optical micrographs of aqueous suspensions of Arkema nanotubes at different weight fractions. Large aggregates form in response to the depletion attractive interactions. Scale: 100 μm .

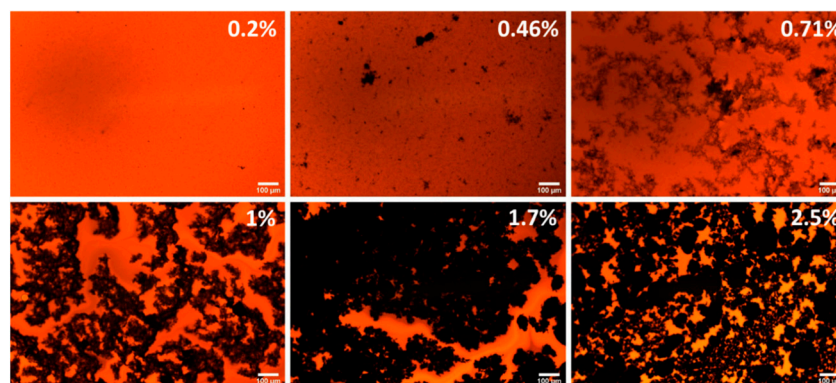


Figure 3. Optical micrographs of aqueous suspensions of Nanocyl nanotubes at different weight fractions. Large aggregates form in response to the depletion attractive interactions. Scale: 100 μm .

The results of electronic conductivity measurements at equilibrium are shown in Figure 4. A typical percolation-type behavior is observed. The conductivity increases by several orders of magnitude at the percolation threshold. These thresholds are about 1 and 1.5 wt% for Nanocyl and Arkema materials, respectively. Particularly high conductivity values are obtained for concentrations above 2 wt% for both materials, approaching 100 ms/cm. Arkema materials are investigated in higher concentrations compared to Nanocyl nanotubes because of their difference in percolation threshold. The difference is likely arising from slight differences in the aspect ratio of the particles after sonication. The lower percolation threshold of Nanocyl nanotubes can be explained by a greater aspect ratio. This expectation is consistent with optical microscope images reported in Figures 2 and 3 where Nanocyl nanotubes tend to form a sample-spanning network of aggregates at a lower weight fraction compared to Arkema ones. As discussed further, the expectation that Nanocyl nanotubes have a greater aspect ratio is also supported by rheological characterizations.

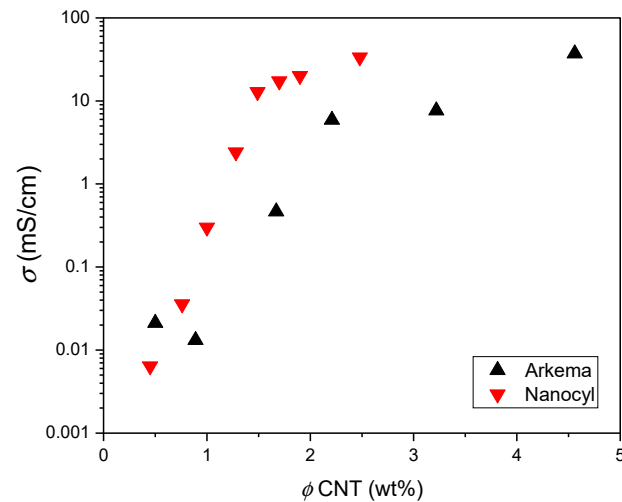


Figure 4. Electronic conductivity of Arkema and Nanocyl suspensions as a function of concentrations of nanotubes (%wt).

Rheological properties of samples with different weight fractions are shown in Figure 5. The presence of MWCNTs results in a clear shear thinning behavior of the suspensions. Shear thinning in nanotube suspensions can arise from the shear-induced alignment of the particles but also from network formation when the particles tend to aggregate [35,36]. Here, the viscosity decreases as a function of shear rate by three orders of magnitude, with an exponent close to -1 , thereby revealing a yield stress fluid behavior. A distinctive feature of these suspensions is their low carbon content and very low consistency index, ensuring that the stress remains near a constant value across a broad range of shear rates. A likely representation of the flow involves the formation of a small number of weak regions that are the locus of rearrangements and fractures that constantly form and heal.

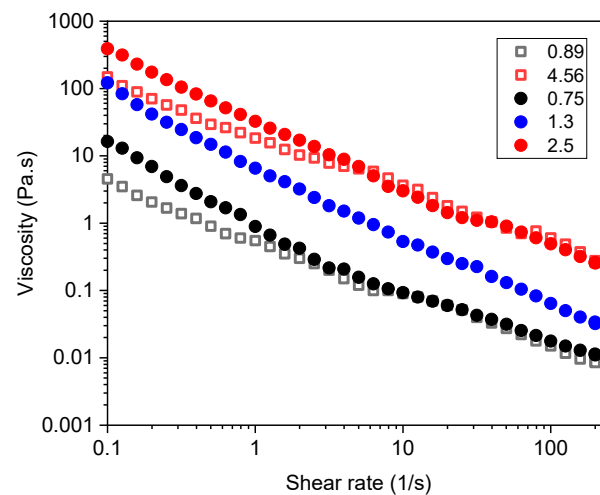


Figure 5. Viscosity as a function of shear rate for suspensions of Arkema (open squares) and Nanocyl (filled circles) MWCNTs. Weight fractions of the samples are indicated in wt% in inset.

This behavior results in interesting effective viscosity properties. The suspensions containing 1.8 wt% of Nanocyl material, which are highly conductive, display an effective viscosity of 1.2 Pa.s for a shear rate of 5 s^{-1} . Even highly concentrated Arkema suspensions with 4.5 wt% of MWCNT still display a limited viscosity of only 6.4 Pa.s at a shear rate of 5 s^{-1} . The present results therefore confirm that the use of thin MWCNTs enables the achievement of highly conductive suspensions with reasonably low apparent viscosity.

In order to confirm the potential interest of the present suspensions for flow electrochemical applications, it remains critical to check their conductivity under shear. Results of conductance measurements in a Couette cell [3] are shown in Figure 6 for Arkema and Nanocyl materials. The conductance, $1/R$, is plotted as a function of shear rate, where R is the resistance measured between the concentric circular electrodes. It is observed that the conductance decreases very slightly for all the investigated MWCNT suspensions. This slight decrease can result from small fractures that allow the flow of the material. The fact that conductivity does not vanish with shear shows that the structural changes in nanotube suspensions remain limited. This is consistent with the description given above of a yield stress fluid with a low consistency index. The material resists the fluidization and disruption of conductive pathways up to shear rates of several hundreds of s^{-1} , even for solid contents as low as 1 wt%.

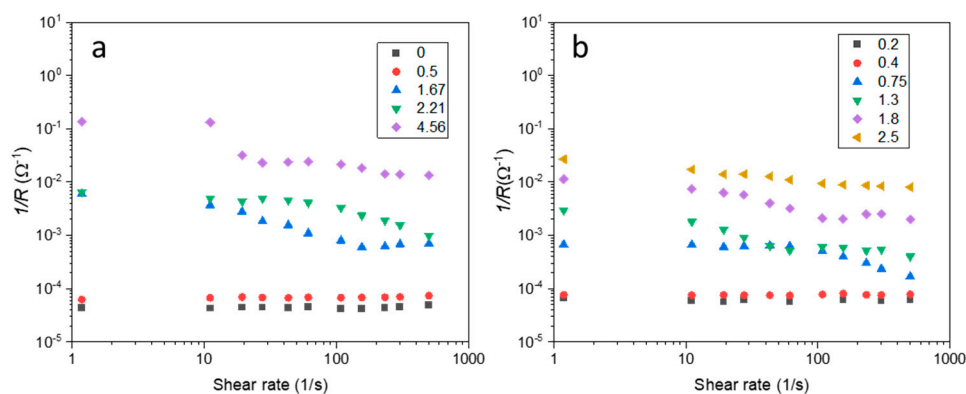


Figure 6. Conductance of aqueous suspensions of Arkema (a) and Nanocyl (b) MWCNTs as a function of shear rate. Weight fractions of the samples are indicated in wt% in inset.

Results of cyclic voltammetry experiments [37] are shown in Figure 7. The current I was measured when the voltage V was varied from -0.5 V to 0.5 V at a scan rate $\left(\frac{dV}{dt}\right)$ of 50 mV/s. The specific gravimetric capacitance C_{sp} is then deduced by normalizing the current measured for $V = 0$ by the weight m of carbon material contained in the volume of the cell. The cell volume in the present setup is 0.24 cm^3 per electrode [3].

$$C_{sp} = \frac{2I}{m \cdot \left(\frac{dV}{dt}\right)}$$

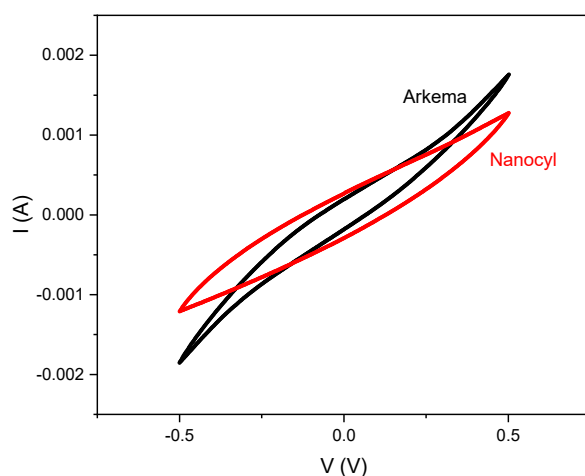


Figure 7. Cyclic voltammetry of suspensions containing 4.5 wt% of Arkema MWCNTs and 1.8 wt% of Nanocyl MWCNTs.

The Arkema suspension containing 4.5 wt% of MWCNT, and the Nanocyl suspension containing 1.8 wt% of MWCNT, respectively, display specific gravimetric capacitance of 2 F/g and 6.5 F/g. These values are not particularly high but comparable to those measured for low-viscosity carbon black suspensions at similar scan rates [3].

4. Conclusions

In conclusion, this study presents a novel approach to address challenges associated with flowable electrodes in electrochemical applications by introducing colloidal suspensions of thin multiwall carbon nanotubes (MWCNTs). The suspensions are stabilized in water with a non-ionic surfactant and are further concentrated through a dialysis process. The used surfactant molecules contain aromatic groups that promote their adsorption at the interface of the nanotubes. The suspensions are homogenized by tip sonication prior to concentration by dialysis. Characterizations of electrical properties demonstrate a percolation-type behavior in electronic conductivity, with a strong increase above a critical concentration of carbon nanotubes. Additionally, the suspensions display a shear-thinning behavior in rheological properties and stable conductance under shear conditions. Clustering of nanotubes is enhanced and conductivity is improved because of weak depletion attractive interactions between the nanotubes. The depletion attraction is attributed to the presence of a large excess of surfactant micelles. Shear induces small structural variations in the depletion-induced aggregates through constant minute structural rearrangements. These reversible rearrangements allow maintaining flow at a nearly constant stress of a globally persistent percolated and conductive network. Optimal suspensions display high conductivity of the order of 50 ms/cm at a low carbon content, below 2 wt%. Cyclic voltammetry experiments reveal specific gravimetric capacitance values comparable to low viscosity carbon black suspensions. This work contributes therefore to advancing the field of flowable electrodes, offering a potential solution to the challenges associated with high viscosity and carbon content. The use of thin MWCNTs in colloidal suspensions presents a promising approach for further developments in flow electrochemical applications, emphasizing the importance of balancing electronic conductivity and viscosity for improved device performance and longevity. Future research directions should focus on enhancing energy storage capabilities and in characterizing these capabilities in flow conditions. At present, using a low carbon content is naturally an intrinsic limitation for achieving high gravimetric capacitance. This limitation can be somehow mitigated using thin carbon nanotubes, but it remains an obstacle. A promising perspective would consist of using pseudo-capacitive flow electrodes by introducing active redox species, such as quinone derivatives, in the formulations. This approach has already been proved to be efficient at increasing performances of flow electrochemical systems [38–42].

Author Contributions: Conceptualization, A.C., N.B. and P.P.; methodology, N.B., W.N. and P.P.; formal analysis, N.B., A.C., J.Y. and P.P.; investigation, M.H., W.N. and X.B.; resources, W.N. and X.B.; writing—original draft preparation, M.H. and P.P.; writing—review and editing, N.B., A.C., J.Y. and P.P.; supervision, N.B., W.N. and P.P.; funding acquisition, N.B., A.C. and P.P. All authors have read and agreed to the published version of the manuscript.

Funding: This work was supported by a public grant overseen by the French National Research Agency (ANR), Project Reference No. ANR19-CE06-0026 (ElectroFluid).

Data Availability Statement: The data that support the findings of this study are available from the corresponding author upon reasonable request.

Conflicts of Interest: The authors declare no conflicts of interest.

References

1. Presser, V.; Dennison, C.R.; Campos, J.; Knehr, K.W.; Kumbur, E.C.; Gogotsi, Y. The Electrochemical Flow Capacitor: A New Concept for Rapid Energy Storage and Recovery. *Adv. Energy Mater.* **2012**, *2*, 895–902. [[CrossRef](#)]
2. Campos, J.W.; Beidaghi, M.; Hatzell, K.B.; Dennison, C.R.; Musci, B.; Presser, V.; Kumbur, E.C.; Gogotsi, Y. Investigation of carbon materials for use as a flowable electrode in electrochemical flow capacitors. *Electrochim. Acta* **2013**, *98*, 123–130. [[CrossRef](#)]

3. Alfonso, M.S.; Parant, H.; Yuan, J.K.; Neri, W.; Laurichesse, E.; Kampioti, K.; Colin, A.; Poulin, P. Highly conductive colloidal carbon based suspension for flow-assisted electrochemical systems. *Science* **2021**, *24*, 102456. [[CrossRef](#)]
4. Yu, F.; Yang, Z.Q.; Cheng, Y.J.; Xing, S.Y.; Wang, Y.Y.; Ma, J. A comprehensive review on flow-electrode capacitive deionization: Design, active material and environmental application. *Sep. Purif. Technol.* **2022**, *281*, 119870. [[CrossRef](#)]
5. Ma, J.J.; Zhang, C.Y.; Yang, F.; Zhang, X.D.; Suss, M.E.; Huang, X.; Liang, P. Carbon Black Flow Electrode Enhanced Electrochemical Desalination Using Single-Cycle Operation. *Environ. Sci. Technol.* **2020**, *54*, 1177–1185. [[CrossRef](#)] [[PubMed](#)]
6. Zhang, C.Y.; Ma, J.X.; Wu, L.; Sun, J.Y.; Wang, L.; Li, T.Y.; Waite, T.D. Flow Electrode Capacitive Deionization (FCDI): Recent Developments, Environmental Applications, and Future Perspectives. *Environ. Sci. Technol.* **2021**, *55*, 4243–4267. [[CrossRef](#)] [[PubMed](#)]
7. Yang, F.; He, Y.F.; Rosentsvit, L.; Suss, M.E.; Zhang, X.R.; Gao, T.; Liang, P. Flow-electrode capacitive deionization: A review and new perspectives. *Water Res.* **2021**, *200*, 117222. [[CrossRef](#)]
8. Jeon, S.I.; Park, H.R.; Yeo, J.G.; Yang, S.; Cho, C.H.; Han, M.H.; Kim, D.K. Desalination via a new membrane capacitive deionization process utilizing flow-electrodes. *Energy Environ. Sci.* **2013**, *6*, 1471–1475. [[CrossRef](#)]
9. Doornbusch, G.J.; Dykstra, J.E.; Biesheuvel, P.M.; Suss, M.E. Fluidized bed electrodes with high carbon loading for water desalination by capacitive deionization. *J. Mater. Chem. A* **2016**, *4*, 3642–3647. [[CrossRef](#)]
10. Yang, S.; Park, H.R.; Yoo, J.; Kim, H.; Choi, J.; Han, M.H.; Kim, D.K. Plate-Shaped Graphite for Improved Performance of Flow-Electrode Capacitive Deionization. *J. Electrochem. Soc.* **2017**, *164*, E480–E488. [[CrossRef](#)]
11. Tang, K.X.; Yiaccoumi, S.; Li, Y.P.; Tsouris, C. Enhanced Water Desalination by Increasing the Electroconductivity of Carbon Powders for High-Performance Flow-Electrode Capacitive Deionization. *ACS Sustain. Chem. Eng.* **2019**, *7*, 1085–1094. [[CrossRef](#)]
12. Rommerskirchen, A.; Linnartz, C.J.; Müller, D.; Willenberg, L.K.; Wessling, M. Energy Recovery and Process Design in Continuous Flow Electrode Capacitive Deionization Processes. *ACS Sustain. Chem. Eng.* **2018**, *6*, 13007–13015. [[CrossRef](#)]
13. Lee, J.H.; Weingarh, D.; Grobelsek, I.; Presser, V. Use of Surfactants for Continuous Operation of Aqueous Electrochemical Flow Capacitors. *Energy Technol.* **2016**, *4*, 75–84. [[CrossRef](#)]
14. Torop, J.; Summer, F.; Zadin, V.; Koiranen, T.; Jänes, A.; Lust, E.; Aabloo, A. Low concentrated carbonaceous suspensions assisted with carboxymethyl cellulose as electrode for electrochemical flow capacitor. *Eur. Phys. J. E* **2019**, *42*, 8. [[CrossRef](#)] [[PubMed](#)]
15. Akuzum, B.; Singh, P.; Eichfeld, D.A.; Agartan, L.; Uzun, S.; Gogotsi, Y.; Kumbur, E.C. Percolation Characteristics of Conductive Additives for Capacitive Flowable (Semi-Solid) Electrodes. *ACS Appl. Mater. Interfaces* **2020**, *12*, 5866–5875. [[CrossRef](#)]
16. Gloukhovski, R.; Suss, M.E. Measurements of the Electric Conductivity of MWCNT Suspension Electrodes with Varying Potassium Bromide Electrolyte Ionic Strength. *J. Electrochem. Soc.* **2020**, *167*, 020528. [[CrossRef](#)]
17. Balmforth, N.J.; Frigaard, I.A.; Ovarlez, G. Yielding to Stress: Recent Developments in Viscoplastic Fluid Mechanics. *Annu. Rev. Fluid Mech.* **2014**, *46*, 121–146. [[CrossRef](#)]
18. Ouyang, L.X.; Wu, Z.H.; Wang, J.; Qi, X.P.; Li, Q.; Wang, J.T.; Lu, S.G. The effect of solid content on the rheological properties and microstructures of a Li-ion battery cathode slurry. *RSC Adv.* **2020**, *10*, 19360–19370. [[CrossRef](#)] [[PubMed](#)]
19. Larsen, T.; Royer, J.R.; Laidlaw, F.H.J.; Poon, W.C.K.; Larsen, T.; Andreasen, S.J.; Christiansen, J.C. Controlling the rheo-electric properties of graphite/carbon black suspensions by ‘flow switching’. *arXiv* **2023**, arXiv:2311.05302. [[CrossRef](#)]
20. Ando, Y.; Zhao, X.; Shimoyama, H.; Sakai, G.; Kaneto, K. Physical properties of multiwalled carbon nanotubes. *Int. J. Inorg. Mater.* **1999**, *1*, 77–82. [[CrossRef](#)]
21. Balberg, I.; Anderson, C.H.; Alexander, S.; Wagner, N. EXCLUDED VOLUME AND ITS RELATION TO THE ONSET OF PERCOLATION. *Phys. Rev. B* **1984**, *30*, 3933–3943. [[CrossRef](#)]
22. Cho, Y.; Yoo, C.Y.; Lee, S.W.; Yoon, H.; Lee, K.S.; Yang, S.; Kim, D.K. Flow-electrode capacitive deionization with highly enhanced salt removal performance utilizing high-aspect ratio functionalized carbon nanotubes. *Water Res.* **2019**, *151*, 252–259. [[CrossRef](#)]
23. Chen, K.Y.; Shen, Y.Y.; Wang, D.M.; Hou, C.H. Carbon nanotubes/activated carbon hybrid as a high-performance suspension electrode for the electrochemical desalination of wastewater. *Desalination* **2022**, *522*, 115440. [[CrossRef](#)]
24. Wang, Z.L.; Hu, Y.D.; Wei, Q.; Li, W.S.; Liu, X.; Chen, F.M. Enhanced Desalination Performance of a Flow-Electrode Capacitive Deionization System by Adding Vanadium Redox Couples and Carbon Nanotubes. *J. Phys. Chem. C* **2021**, *125*, 1234–1239. [[CrossRef](#)]
25. Petek, T.J.; Hoyt, N.C.; Savinell, R.F.; Wainright, J.S. Characterizing Slurry Electrodes Using Electrochemical Impedance Spectroscopy. *J. Electrochem. Soc.* **2016**, *163*, A5001–A5009. [[CrossRef](#)]
26. Cohen, H.; Eli, S.E.; Jogi, M.; Suss, M.E. Suspension Electrodes Combining Slurries and Upflow Fluidized Beds. *ChemSusChem* **2016**, *9*, 3045–3048. [[CrossRef](#)]
27. Vigolo, B.; Coulon, C.; Maugey, M.; Zakri, C.; Poulin, P. An experimental approach to the percolation of sticky nanotubes. *Science* **2005**, *309*, 920–923. [[CrossRef](#)]
28. Chiodarelli, N.; Richard, O.; Bender, H.; Heyns, M.; De Gendt, S.; Groeseneken, G.; Vereecken, P.M. Correlation between number of walls and diameter in multiwall carbon nanotubes grown by chemical vapor deposition. *Carbon* **2012**, *50*, 1748–1752. [[CrossRef](#)]
29. Lucas, A.; Zakri, C.; Maugey, M.; Pasquali, M.; van der Schoot, P.; Poulin, P. Kinetics of Nanotube and Microfiber Scission under Sonication. *J. Phys. Chem. C* **2009**, *113*, 20599–20605. [[CrossRef](#)]
30. Pagani, G.; Green, M.J.; Poulin, P.; Pasquali, M. Competing mechanisms and scaling laws for carbon nanotube scission by ultrasonication. *Proc. Natl. Acad. Sci. USA* **2012**, *109*, 11599–11604. [[CrossRef](#)] [[PubMed](#)]

31. Parant, H.; Muller, G.; Le Mercier, T.; Tarascon, J.M.; Poulin, P.; Colin, A. Flowing suspensions of carbon black with high electronic conductivity for flow applications: Comparison between carbons black and exhibition of specific aggregation of carbon particles. *Carbon* **2017**, *119*, 10–20. [[CrossRef](#)]
32. Simsek, Y.; Ozyuzer, L.; Seyhan, A.; Tanoglu, M.; Schulte, K. Temperature dependence of electrical conductivity in double-wall and multi-wall carbon nanotube/polyester nanocomposites. *J. Mater. Sci.* **2007**, *42*, 9689–9695. [[CrossRef](#)]
33. Kyrylyuk, A.V.; van der Schoot, P. Continuum percolation of carbon nanotubes in polymeric and colloidal media. *Proc. Natl. Acad. Sci. USA* **2008**, *105*, 8221–8226. [[CrossRef](#)]
34. Mao, Y.; Cates, M.E.; Lekkerkerker, H.N.W. Depletion force in colloidal systems. *Phys. A* **1995**, *222*, 10–24. [[CrossRef](#)]
35. Nadiv, R.; Fernandes, R.M.F.; Ochbaum, G.; Dai, J.; Buzaglo, M.; Varenik, M.; Biton, R.; Furó, I.; Regev, O. Polymer nanocomposites: Insights on rheology, percolation and molecular mobility. *Polymer* **2018**, *153*, 52–60. [[CrossRef](#)]
36. Fan, Z.; Advani, S.G. Rheology of multiwall carbon nanotube suspensions. *J. Rheol.* **2007**, *51*, 585–604. [[CrossRef](#)]
37. Faulkner, L.R.; Bard, A.J. (Eds.) *Electrochemical Methods: Fundamentals and Applications*, 2nd ed.; Wiley: Hoboken, NJ, USA, 2000; ISBN 978-0-471-04372-0.
38. Hatzell, K.B.; Beidaghi, M.; Campos, J.W.; Dennison, C.R.; Kumbur, E.C.; Gogotsi, Y. A high performance pseudocapacitive suspension electrode for the electrochemical flow capacitor. *Electrochim. Acta* **2013**, *111*, 888–897. [[CrossRef](#)]
39. Hou, S.J.; Wang, M.; Xu, X.T.; Li, Y.D.; Li, Y.J.; Lu, T.; Pan, L.K. Nitrogen-doped carbon spheres: A new high-energy-density and long life pseudo-capacitive electrode material for electrochemical flow capacitor. *J. Colloid Interface Sci.* **2017**, *491*, 161–166. [[CrossRef](#)]
40. Hunt, C.; Matthejat, M.; Anderson, C.; Sepunaru, L.; Ménard, G. Symmetric Phthalocyanine Charge Carrier for Dual Redox Flow Battery/Capacitor Applications. *ACS Appl. Energy Mater.* **2019**, *2*, 5391–5396. [[CrossRef](#)]
41. Tomai, T.; Saito, H.; Honma, I. High-energy-density electrochemical flow capacitors containing quinone derivatives impregnated in nanoporous carbon beads. *J. Mater. Chem. A* **2017**, *5*, 2188–2194. [[CrossRef](#)]
42. Yoon, H.; Kim, H.J.; Yoo, J.J.; Yoo, C.Y.; Park, J.H.; Lee, Y.A.; Cho, W.K.; Han, Y.K.; Kim, D.H. Pseudocapacitive slurry electrodes using redox-active quinone for high-performance flow capacitors: An atomic-level understanding of pore texture and capacitance enhancement. *J. Mater. Chem. A* **2015**, *3*, 23323–23332. [[CrossRef](#)]

Disclaimer/Publisher’s Note: The statements, opinions and data contained in all publications are solely those of the individual author(s) and contributor(s) and not of MDPI and/or the editor(s). MDPI and/or the editor(s) disclaim responsibility for any injury to people or property resulting from any ideas, methods, instructions or products referred to in the content.